CHEMISTRY
A EUROPEAN JOURNAL

ChemPubSoc
Europe

DOI: 10.1002/chem.201202645

Amycolamicin: A Novel Broad-Spectrum Antibiotic Inhibiting Bacterial Topoisomerase

Ryuichi Sawa,[a] Yoshiaki Takahashi,[b] Hideki Hashizume,[a] Kazushige Sasaki,[b] Yoshimasa Ishizaki,[a] Maya Umekita,[a] Masaki Hatano,[a] Hikaru Abe,[a] Takumi Watanabe,[a] Naoko Kinoshita,[a] Yoshiko Homma,[a] Chigusa Hayashi,[a] Kunio Inoue,[a] Syunichi Ohba,[c] Toru Masuda,[c] Masayuki Arakawa,[a] Yoshihiko Kobayashi,[b] Masa Hamada,[a] Masayuki Igarashi,[a] Hayamitsu Adachi,*[a] Yoshio Nishimura,[a] and Yuzuru Akamatsu[a]

Abstract: The abuse of antibacterial drugs imposes a selection pressure on bacteria that has driven the evolution of multidrug resistance in many pathogens. Our efforts to discover novel classes of antibiotics to combat these pathogens resulted in the discovery of amycolamicin (AMM). The absolute structure of AMM was determined by NMR spectroscopy, X-ray analysis, chemical degradation, and modification of its functional groups. AMM consists of *trans*-decalin, tetramic acid, two unusual sugars (amycolose and amykitanose), and dichloropyrrole carboxylic acid. The pyranose ring named as amykitanose undergoes anomerization in methanol. AMM is a potent and broad-spectrum antibiotic against Gram-positive pathogenic bacteria by inhibiting DNA gyrase and bacterial topoisomerase IV. The target of AMM has been proved to be the DNA gyrase B subunit and its binding mode to DNA gyrase is different from those of novobiocin and coumermycin, the known DNA gyrase inhibitors.

Keywords: antibiotics · DNA replication · natural products · structure elucidation

Introduction

The emergence and widespread frequency of multiple drug-resistant bacteria have made the treatment of bacterial infectious diseases increasingly difficult. In nosocomial infections, methicillin-resistant *Staphylococcus aureus* (MRSA) is one of the most problematic pathogens where vancomycin (VAN) is used as the last resort. However, overuse of VAN has enhanced the widespread development of vancomycin-intermediate-resistant *S. aureus*.[1] Moreover, VAN-resistant *S. aureus* (VRSA) and VAN-resistant *Enterococcus faecalis*/*faecium* (VRE) have been a widespread problem in nosocomial infections.[2,3] Community-acquired pneumonia is one of the most serious infections caused by *Streptococcus pneumoniae* and *Haemophilus influenzae*.[4] Drug-resistant strains are also increasingly isolated from patients and are known as penicillin-resistant *S. pneumoniae* (PRSP),[5–7] macrolide-resistant *S. pneumoniae* (MRSP), and beta-lactamase-negative ampicillin-resistant (BLNAR) and beta-lactamase-positive amoxicillin-clavulanate-resistant (BLPACR) strains of *H. influenzae*.[8]

In order to combat the growing number of drug-resistant pathogens, synthetic tailoring of natural antibiotics has been widely carried out to create a next generation of antibiotics. New generation antibiotics are often designed to inhibit the activity of pathogens that have gained resistance to the previous generation ones. For example, second- and third-generation quinolones like ciprofloxacin and levofloxacin are far more active against the resistant strains of pathogen-mutated DNA gyrase and topoisomerase IV by appropriate functionalization of the quinolone scaffold.[9,10] Improvements of existing scaffolds are a good short-term strategy for refilling the antibiotic pipeline.

On the other hand, discovery of new antibiotic scaffolds from natural products would be a more sustainable way to overcome resistant strains, leading to unprecedented structure diversity and a greater chance for biological activity. Unfortunately, development and approval of new antibiotics from natural products has not caught up with the emergence

[a] Dr. R. Sawa, Dr. H. Hashizume, Dr. Y. Ishizaki, M. Umekita, Dr. M. Hatano, H. Abe, Dr. T. Watanabe, N. Kinoshita, Y. Homma, C. Hayashi, K. Inoue, Dr. M. Arakawa, Dr. M. Hamada, Dr. M. Igarashi, Dr. H. Adachi, Dr. Y. Nishimura, Dr. Y. Akamatsu
Institute of Microbial Chemistry (BIKAKEN), Tokyo
3-14-23, Kamiosaki, Shinagawa-ku
Tokyo 141-0021 (Japan)
Fax: (+81) 3-3441-7589
E-mail: adachih@bikaken.or.jp

[b] Dr. Y. Takahashi, Dr. K. Sasaki, Dr. Y. Kobayashi
Institute of Microbial Chemistry (BIKAKEN), Hiyoshi
3-34-17, Ida, Nakahara-ku, Kawasaki-shi
Kanagawa 211-0035 (Japan)

[c] S. Ohba, T. Masuda
Institute of Microbial Chemistry (BIKAKEN), Numazu
18-24, Miyamoto, Numazu-shi, Shizuoka 410-0301 (Japan)

Supporting information for this article is available on the WWW under http://dx.doi.org/10.1002/chem.201202645.

of drug-resistant pathogens. As well, the discovery of new scaffolds has been decreasing year by year due to an increase in known scaffold rediscovery.

In order to effectively eliminate the rediscovery of known scaffolds during antibiotic screening of microbial metabolites, we used many types of clinical isolates, passaged-resistant strains, and genetically modified strains as test organisms to observe the cross-resistance. In the course of our screening, we discovered a new broad-spectrum antibiotic named amycolamicin (AMM, Figure 1) from the culture broth of

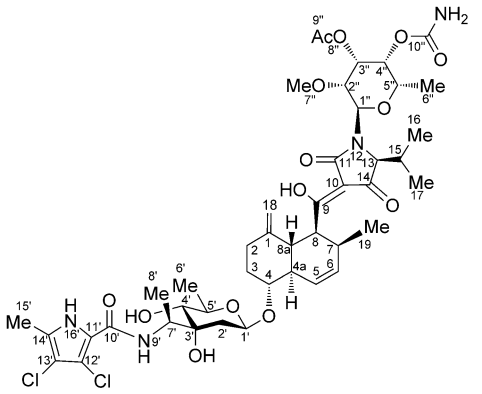

Figure 1. Structure of AMM.

the soil actinomycete, *Amycolatopsis* sp. MK575-fF5 and patented AMM in 2009. The chemical structure of AMM was determined by NMR spectroscopy, chemical degradation, X-ray analysis, and modification of its functional groups. AMM has a unique structure consisting of *trans*-decalin, tetramic acid, two unusual sugars (amycolose and amykitanose), and 3, 4-dichloro-1*H*-pyrrole-2-carboxylic acid. AMM shows potent antibacterial activity against Gram-positive bacteria including PRSP, MRSA, and VRE and some Gram-negative bacteria, including BLNAR and BLPACR strains of *H. influenzae*.

Decatromicin B,[11] pyrrolosporin A,[12] and kibdelomycin,[13] which are related to AMM, all show potent antibacterial activity against pathogenic Gram-positive bacteria. These antibiotics possess a common pyrrolamide-sugar-decalin ring scaffold. In particular, the pyrrolamides have recently been identified as a new class of antibacterial agents that inhibit the activity of DNA gyrase, resulting in inhibition of DNA synthesis leading to bacterial cell death.[14]

The characteristic structure and promising antibacterial activities of AMM have led us to clarify the absolute structure and the mode of action of AMM in order to encourage further drug development and design of new AMM derivatives. Herein, we describe the isolation, absolute structure, structural isomerization, biological activities, and mode of action of AMM.

Results

Fermentation and isolation of amycolamicin: The producing organism, *Amycolatopsis* sp. MK575-fF5, was grown in liquid culture for four days and 80 L of the fermentation broth were separated into the mycelial cake (2.5 kg) and the supernatant. AMM was purified by successive steps of extraction from the mycelia followed by gel filtration and silica gel chromatography. Active fractions were collected and concentrated in vacuo to give a pale orange solid (827 mg). A small amount of the solid (54 mg) was purified by reversed-phase HPLC developed with a linear gradient of 50% aqueous MeOH to 100% MeOH for 75 min. The fractions containing pure AMM analyzed by HPLC were collected to give a white solid. Finally the solid was suspended in ethyl acetate and washed with phosphate buffer (pH 7.0) and aqueous HCl solution to give a free form of AMM (34 mg).

Structural features and absolute structure of amycolamicin: AMM is soluble in $CHCl_3$, MeOH, DMSO, and acetone, but insoluble in H_2O. The specific rotation of AMM fluctuated depending on the isolation conditions. AMM isolated by HPLC showed a specific rotation of $[\alpha]_D^{20} = -20.6°$ in MeOH, whereas it exhibited $[\alpha]_D^{23} = -36.5°$ after washing an ethyl acetate solution of AMM with phosphate buffer and aqueous HCl solution. The UV spectrum of AMM has a characteristic absorption maxima at $\lambda = 280$ nm ($\log\varepsilon = 4.45$) in acidic MeOH and has a hypsochromic shift to $\lambda = 248$ ($\log\varepsilon = 4.30$) and 277 nm ($\log\varepsilon = 4.45$) in alkaline MeOH. The molecular formula of AMM was found to be $C_{44}H_{60}Cl_2N_4O_{14}$ by HRESI-MS. The ^{1}H NMR spectrum of AMM showed major and minor species in a ratio of 2:1 in $CDCl_3$ (Figure S2 in the Supporting Information). The spectra in [D$_4$]MeOH gave simplified NMR signals originating from a single species, but not all signals of the ^{1}H and ^{13}C NMR spectra were observed (Figures S11 and S12 in the Supporting Information). Furthermore, new species appeared gradually over time as shown in Figure S14 in the Supporting Information.

Various NMR spectra in $CDCl_3$ were extensively analyzed for structural determination purposes because they had sharper signals and some exchangeable protons were available for structural analysis even in a mixture of major and minor forms originating from the tautomerization of the tetramic acid moiety. The ^{1}H and ^{13}C NMR data of the major form are summarized in Table 1. The ^{13}C NMR and DEPT spectra revealed that AMM has 44 carbon atoms, comprised of twelve quaternary sp^2 carbon atoms, including carbonyl atoms, one quaternary sp^3 carbon atom, two sp^2 methine carbon atoms, sixteen sp^3 methine carbon atoms, one sp^2 methylene carbon atom, three sp^3 methylene carbon atoms, and nine methyl carbon atoms.

The structure of AMM was elucidated mainly by using two-dimensional NMR spectroscopy. The proton signals without C–H correlations in the ^{1}H–^{13}C HMQC spectrum were assigned to two NH groups ($\delta = 6.64$ (NH-9′) and 9.73 ppm (NH-16′)) and one NH_2 group ($\delta = 4.79$ ppm (NH_2-10″)), confirmed by ^{1}H–^{15}N HMQC spectroscopy.

The ^{1}H–^{1}H COSY spectrum showed four partial structures, amycolose (I),[15] decalin (II), the isopropyl group of

Table 1. ^{1}H and ^{13}C NMR data of AMM measured in $CDCl_3$.[a]

Position	δ_C [ppm]		δ_H [ppm]	Multiplet, J [Hz]	Position	δ_C [ppm]		δ_H [ppm]	Multiplet, J [Hz]
1	149.7	−C=			5′	70.5	−CH−	3.59	dq 6.2, 9.1
2	34.3	$-CH_2-$	2.12, 2.32	m, m	6′	18.1	$-CH_3$	1.32	d 6.1
3	33.9	$-CH_2-$	1.32, 2.24	m, m	7′	52.6	−CH−	4.41	quintet 7.0
4	77.7	−CH−	3.59	dt 4.7, 10.3	8′	16.2	$-CH_3$	1.30	d 7.0
4a	48.0	−CH−	1.90	td 10.3, 1.5	NH-9′			6.64	d 7.1
5	125.9	=CH−	6.01	dt 10.0, 1.5	10′	161.4	−C=		
6	130.9	=CH−	5.63	ddd 2.5, 4.2, 10.0	11′	117.4	−C=		
7	32.2	−CH−	2.60	m	12′	112.4	−C=		
8	42.4	−CH−	4.10	dd 6.3, 12.0	13′	111.0	−C=		
8a	37.3	−CH−	2.34	m	14′	128.8	−C=		
9	191.4	−C=			15′	11.4	$-CH_3$	2.28	s
10	102.5	−C=			NH-16′			9.73	brs
11	175.6	−C=			1″	76.2	−CH−	5.01	d 8.5
13	71.2	−CH−	3.79	d 3.0	2″	74.3	−CH−	4.27	dd 3.2, 8.5
14	193.5	−C=			3″	67.8	−CH−	5.93	t 3.3
15	30.5	−CH−	2.23	m	4″	68.6	−CH−	5.03	dd 3.3, 6.1
16	15.8	$-CH_3$	0.94	d 6.9	5″	70.5	−CH−	4.40	m
17	17.9	$-CH_3$	1.19	d 7.0	6″	13.9	$-CH_3$	1.41	d 6.8
18	105.2	$=CH_2$	4.39, 4.67	brs, brs	7″	57.4	−CH−	3.31	s
19	17.9	$-CH_3$	0.89	d 7.2	8″	170.0	−C=		
1′	95.4	−CH−	4.90	dd 1.8, 9.2	9″	21.1	$-CH_3$	2.17	s
2′	36.9	$-CH_2-$	1.54	dd 9.2, 12.9	10″	155.2	−C=		
			1.83	d 12.9					
3′	76.5	−C−			NH_2-10″			4.79	brs
4′	74.1	−CH−	3.17	d 9.0					

[a] Chemical shifts are given in [ppm] with tetramethylsilane as internal standard.

tetramic acid (III), and a pyranose named as amykitanose (IV) as shown by the bold lines in Figure 2A.

The connectivities of these partial structures were established by HMBC spectroscopy. The C–H long range couplings from the exo-methylene of H-18a ($\delta = 4.39$ ppm) and H-18b ($\delta = 4.67$ ppm) to C-1 ($\delta = 149.7$ ppm), C-2 ($\delta = 34.3$ ppm), and C-8a ($\delta = 37.3$ ppm) revealed the presence of the decalin ring. The long range couplings from the H-8 ($\delta = 4.10$ ppm) of the decalin ring to the characteristic carbon signals at C-9 ($\delta = 191.4$ ppm) and C-10 ($\delta = 102.5$ ppm) and from H-13 ($\delta = 3.79$ ppm) of the isopropyl group to C-11 ($\delta = 175.6$ ppm) and C-14 ($\delta = 193.5$ ppm), suggested a tetramic acid moiety attached to the C-8 ($\delta = 42.4$ ppm) of the decalin ring. The chemical shifts of the tetramic acid moiety were in good agreement with those of the corresponding signals of a related compound.[16,17]

The long range couplings from H-1″ ($\delta = 5.01$ ppm) to C-5″ ($\delta = 70.5$ ppm), from H-5″ ($\delta = 4.40$ ppm) to C-1″ ($\delta = 76.2$ ppm), from H-2″ ($\delta = 4.27$ ppm) to C-7″ ($\delta = 57.4$ ppm) for the methoxy group, from H-9″ ($\delta = 2.17$ ppm) to C-8″ ($\delta = 170.0$ ppm), from H-3″ ($\delta = 5.93$ ppm) to C-8″ for the acetoxy group connected to C-3″ ($\delta = 67.8$ ppm) of the oxymethine, from the amino proton of NH_2-10″ ($\delta = 4.79$ ppm) to C-10″ ($\delta = 155.2$ ppm), from H-4″ ($\delta = 5.03$ ppm) to C-10″

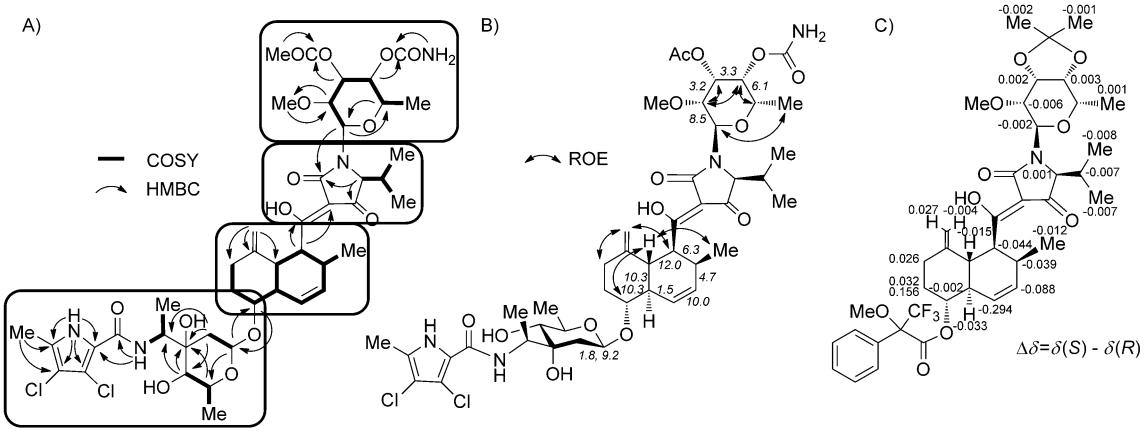

Figure 2. Structure determination of AMM. A) Key correlations of AMM obtained by ^{1}H–^{1}H COSY and HMBC spectroscopy. B) Key correlations of AMM obtained by ROEs and coupling constants. C) $\Delta\delta$ values of **6a** and **6b** for the determination of the stereochemistry at C-4 with a modified Mosher's method.

for the carbamoyl group, from H-1″ to C-11 and the chemical shift of C-1″ ($\delta = 76.2$ ppm) established the linkage of 3-*O*-acetyl-4-*O*-carbamoyl-6-deoxy-2-*O*-methyl-hexopyranose to the N-12 of the tetramic acid by an *N*-glycosidic linkage.

The structure of the amycolose moiety was also elucidated. The correlations from H-1′ ($\delta = 4.90$ ppm) to C-5′ ($\delta = 70.5$ ppm) and from both H-2′$_{eq}$ ($\delta = 1.83$ ppm) and H-5′ ($\delta = 3.59$ ppm) to C-3′ ($\delta = 76.5$ ppm), and from both H-2′$_{eq}$ and H-4′ ($\delta = 3.17$ ppm) to C-7′ ($\delta = 52.6$ ppm) established the amycolose moiety as described in the previous report.[15] Furthermore, the long range couplings observed from NH-9′ ($\delta = 6.64$ ppm) to C-10′ ($\delta = 161.4$ ppm) and C-11′ ($\delta = 117.4$ ppm), from NH-16′ ($\delta = 9.73$ ppm) to C-11′, C-12′ ($\delta = 112.4$ ppm), C-13′ ($\delta = 111.0$ ppm), and C-14′ ($\delta = 128.8$ ppm), from H-15′ ($\delta = 2.28$ ppm) to C-13′ and C-14′ established that 5-methyl-1*H*-pyrrole-2-carboxylic acid was attached to the aminoethyl group of the amycolose by an amide linkage. Observation of the cross peaks from H-1′ to C-4 ($\delta = 77.7$ ppm) of the oxymethine and from H-4 ($\delta = 3.59$ ppm) to C-1′ ($\delta = 95.4$ ppm) indicated the connection of amycolose to the decalin ring by an *O*-glycosidic linkage. All of these correlation data and the fragment ion from HRESI-MS data (*m*/*z* calcd for $[C_{14}H_{19}Cl_2N_2O_4-H_2O]^+$: 331.0611; found: 331.0616) also suggested that the remaining chlorine atoms should be attached to C-12′ and C-13′ on the pyrrole ring as shown in Figure S1 in the Supporting Information. The planar structure of AMM was determined as shown in Figure 2 A.

The relative stereochemistry of the decalin ring and the amykitanose moiety of AMM was successfully elucidated by the analyses of ROE spectra (Figures S9 and S10 in the Supporting Information). ROEs were observed between H-4 and H-8a, H-4a ($\delta = 1.90$ ppm) and H-8, H-8a ($\delta = 2.34$ ppm) and H-19 ($\delta = 0.89$ ppm), H-18a and H-2, H-18b and H-8, hence establishing a *trans*-decalin skeleton as shown in Figure 2 B. For amykitanose with bulky groups at C-2″, C-3″, and C-4″, the correlation between H-1″ and H-6″ ($\delta = 1.41$ ppm), H-2″ and H-3″, H-2″ and H-4″, H-4″ and H-5″, respectively in the 1D ROE spectra together with proton–proton couplings of $^3J_{1,2} = 8.5$, $^3J_{2,3} = 3.2$, $^3J_{3,4} = 3.3$, $^3J_{4,5} = 6.1$, and $^3J_{5,6} = 6.8$ Hz confirmed its structure as 3-*O*-acetyl-4-*O*-carbamoyl-6-deoxy-2-methyl-β-D/α-L-talopyranoside as shown in Figure 2 B.

The absolute stereochemistry of AMM was clarified by a combination of additional NMR analysis and a degradation study (Figure 3). Acidic methanolysis of AMM with concentrated aqueous HCl in MeOH at 50 °C for one hour gave the aglycon **2** and an anomeric mixture of the methyl glycoside of the amycolose-pyrrolecarboxamide (**3α** and **3β**).[15] The anomers **3α** and **3β** were separated and **3β** was crystallized from MeOH to give a colorless crystal. The crystal was subjected to X-ray crystallographic analysis and the absolute

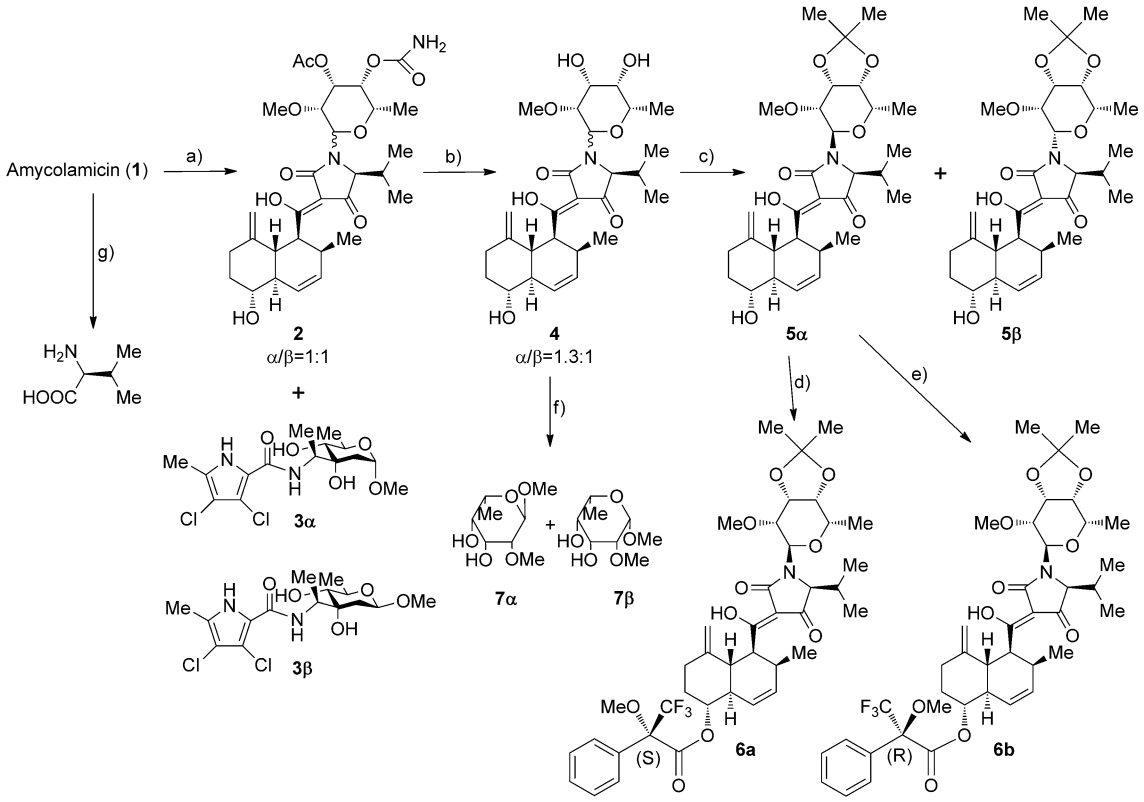

Figure 3. Degradation study of AMM. Reagents and conditions: a) aqueous solution of HCl (10 M), MeOH; b) K_2CO_3 (0.2 M), MeOH; c) 2,2-dimethoxypropane, *p*-toluenesulfonic acid, DMF; d) (*R*)-MTPA-Cl (MTPA = methoxy(trifluoromethyl)phenylacetic acid), Et_3N, 4-dimethylaminopyridine (DMAP), CH_2Cl_2; e) (*S*)-MTPA-Cl, Et_3N, DMAP, CH_2Cl_2; f) 10% HCl/MeOH, 60 °C; g) $NaIO_4$, aqueous solution of HCl (6 M).

structure of the amycolose portion of **3β** was determined to be (2*R*,3*R*,4*R*,6*R*)-4-((*S*)-1-aminoethyl)-6-methoxy-2-ethyltetrahydro-*2H*-pyran-3,4-diol as shown in Figure S18 in the Supporting Information.

The ^{1}H and ^{13}C NMR spectra of compound **2** were complicated spectra similar to the ones of AMM in [D$_4$]MeOH or [D$_6$]acetone (Figures S16 and S17 in the Supporting Information). This was due to the tautomeric feature of the tetramic acid and anomerization of the C-1″ of the amykitanose. The NMR spectrum of compound **2** in [D$_6$]acetone showed the presence of two tautomers of the tetramic acid and anomers of the amykitanose at C-1″, whereas in [D$_4$]MeOH only an anomeric mixture was observed (α/β = 1:1).

A similar phenomenon of anomerization was also observed in a solution of AMM in MeOH. The initial simplified ^{1}H NMR spectrum of the amykitanose moiety gradually changed over time as shown in Figures S11 and S14 in the Supporting Information, and this was also supported by LC-MS analysis (Figure 4A). The analyses of the 1D ROE spec-

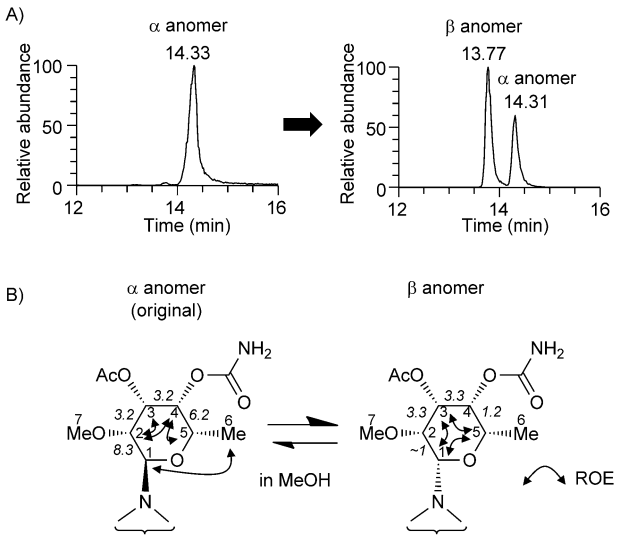

Figure 4. Behavior of a solution of AMM in MeOH. A) LC-MS analyses of a solution of AMM in MeOH. Each chart shows an extracted ion chromatograph of a protonated molecule (*m*/*z* 939.3406–939.3594) of AMM. B) ^{3}J(H,H) values and ROE analyses of AMM in [D$_4$]MeOH.

tra of newly observed additional signals of AMM in [D$_4$]MeOH showed ROE correlations between H-1″ (δ = 5.54 ppm) and H-3″ (δ = 5.12 ppm), H-1″ and H-5″ (δ = 3.92 ppm), H-2″ (δ = 3.78 ppm) and H-7″ (δ = 3.56 ppm), and H-3″ and H-5″, suggesting the presence of an equilibrium of α and β anomers as shown in Figure 4B (see also Figures S13 and S15 in the Supporting Information).

In order to avoid the complexity of the NMR spectra due to anomerization of the sugar moiety of **2**, the 3″,4″-di-*O*-acyl groups were replaced by an *O*-isopropylidene group to yield a simplified ^{1}H NMR spectrum of compound **5α** in [D$_5$]pyridine. Treatment of compound **2** with a 0.2 M solution of K_2CO_3 in MeOH at 60 °C for one hour gave an anomeric mixture of the 3″,4″-di-*O*-deacylaglycon **4**. Treatment of compound **4** with 2, 2-dimethoxypropane in DMF in the presence of *p*-toluenesulfonic acid gave a separable anomeric mixture of the 3″,4″-*O*-isopropylidene derivatives **5α** and **5β**.

Compound **5α** was subjected to the modified Mosher's method.[18] Both the (±)-MTPA esters (**6a** and **6b**) were prepared and analyzed by ^{1}H NMR spectroscopy (Figures S23 and S25 in the Supporting Information). The Δδ values of the corresponding protons indicated that the absolute configuration at C-4 is (*R*). Thus, the stereochemistry of the five asymmetric centers of the *trans*-decalin ring was determined to be (4*R*), (4a*R*), (7*S*), (8*S*), and (8a*R*) as shown in Figure 2C.

Methanolysis of compound **4** under acidic conditions at 60 °C gave anomeric isomers (**7α** and **7β**) of methyl glycoside. The absolute stereochemistry of the sugar was determined by comparing its specific rotation with that of a synthetic compound prepared from the methyl 3,4-*O*-isopropylidene-α-L-fucopyranoside (**8**)[19,20] through four steps as shown in Scheme S1 in the Supporting Information. Oxidation of compound **8** with pyridinium dichlorochromate gave the 2-ulose **9** (92%), which was reduced with $LiAlH_4$ to give the α-L-talopyranoside **10** (major) and its epimer **11** (minor). Methylation of compound **10** with methyl iodide gave the 2-*O*-methyl derivative **12** (96%). Deacetonation of **12** with an aqueous solution of acetic acid (80%) afforded the methyl 6-deoxy-2-*O*-methyl-α-L-talopyranoside **13** (99%). ^{1}H and ^{13}C NMR spectra and specific rotation of the natural methyl glycoside **7α** ($[\alpha]_D^{24} = -74.7°$) were in fair agreement with those of the synthetic compound **13** ($[\alpha]_D^{22} = -75°$). Therefore, the amykitanose moiety of AMM was determined to be the N-linked 3-*O*-acetyl-4-*O*-carbamoyl-6-deoxy-2-*O*-methyl-α-L-talopyranoside, which is a novel sugar. Thus, the stereochemistry at the C-5″ of the amykitanose moiety of AMM[15] was revised.

The stereochemistry at the C-13 in the five-membered ring of the tetramic acid moiety was determined by using a known method.[21] AMM was degraded by periodate oxidation and acid hydrolysis to obtain valine, whose absolute structure was determined to be (*S*) by the advanced Marfey's method[22] (see Figure S35 in the Supporting Information). All of these data helped to establish the absolute structure of AMM as shown in Figure 1.

Amycolamicin exhibits potent antibacterial activity against Gram-positive and some Gram-negative bacteria: AMM showed very potent antibacterial activity against methicillin-sensitive *Staphylococcus aureus* (MSSA), methicillin-resistant *S. aureus* (MRSA), and quinolone-resistant *S. aureus* (QRSA) with minimum inhibitory concentrations (MICs) of 0.125–2, 0.125–1, and 0.25–1 μg mL^{-1}, respectively, as shown in Table S2 in the Supporting Information. AMM also had potent antibacterial activity against other Gram-positive pathogenic bacteria such as *Enterococcus faecalis*, *E. faecium*, and *Streptococcus pneumoniae*, including their drug-resistant strains such as vancomycin-resistant enterococci (VRE) and penicillin-resistant *S. pneumoniae* (PRSP), with

Table 2. Antimicrobial activity of AMM.

Tested strain		MIC [μg mL^{-1}]	Tested strain		MIC [μg mL^{-1}]
Staphylococcus aureus	FDA209P	0.25	*Escherichia coli*	NIHJ	8
St. aureus	Smith	0.25	*Shigella dysenteriae*	JS11910	8
St. aureus	MRSA No.5	0.5	*Sh. flexneri*	4b JS11811	32
St. aureus	MRSA No.17	0.5	*Salmonella enteritidis*	1891	32
St. aureus	MS16526 (MRSA)	1.0	*Proteus vulgaris*		16
St. aureus	TY-04282 (MRSA)	0.5	*Pr. mirabilis*		8
Enterococcus faecalis	JCM 5803	0.25	*Serratia marcescens*		32
Ent. faecalis	NCTC12201 (VRE, *vanA* type)	0.25	*Pseudomonas aeruginosa*	A3	8
Ent. faecalis	NCTC12203 (VRE, *vanA* type)	0.25	*Klebsiella pneumoniae*	PCI602	8
Ent. faecium	JCM 5804	1.0			
Ent. faecium	NCTC12202 (VRE, *vanA* type)	0.5	*Mycobacterium smegmatis*	ATCC607	>64
Ent. faecium	NCTC12204 (VRE, *vanA* type)	0.5	*Candida albicans*	3147	>64

MICs of 0.25–1 μg mL^{-1} (Tables 2 and S3 in the Supporting Information). AMM showed moderate antibacterial activity against some pathogenic Gram-negative bacteria such as *Escherichia coli*, *Shigella dysenteriae*, *Proteus mirabilis*, *Pseudomonas aeruginosa*, and *Klebsiella pneumoniae* with MICs of 8 μg mL^{-1}. AMM did not exhibit antibacterial and antifungal activity against *Mycobacterium smegmatis* and *Candida albicans* even at doses of 64 μg mL^{-1} (Table 2). As shown in Table S3 in the Supporting Information, AMM also exhibited potent antibacterial activity against *H. influenzae*, including its drug-resistant strains such as BLNAR and BLPACR with MICs of 0.5–2 μg mL^{-1}.

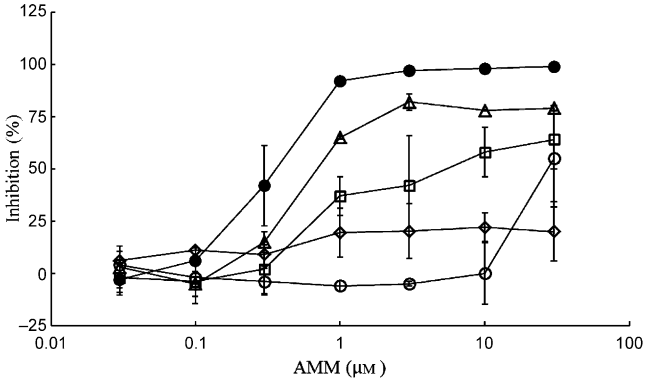

Figure 5. Inhibition of the macromolecular biosynthesis by AMM in the *S. aureus* Smith strain. The inhibitory percentages of the incorporation of DNA ([methyl-^{3}H] thymidine, solid circles), RNA ([5,6-^{3}H] uridine, open triangles), protein (L-[4,5-^{3}H] leucine, open squares), fatty acid (1-^{14}C acetate, open circles), and cell wall ([1-^{3}H] GlcNAc, open diamonds) after incubation for 10 min are plotted against the drug concentration.

Amycolamicin inhibited DNA synthesis in a precursor incorporation study: The attractive broad-spectrum antibacterial activity of AMM prompted us to evaluate its mode of action. In a precursor incorporation study, AMM strongly inhibited the biosynthesis of DNA with an IC_{50} of 0.3 μM, proportional to its MIC against *S. aureus* Smith (Figure 5). The effects of AMM in this assay were similar to those of novobiocin (NOV), a DNA-synthesis inhibitor.[23] At a dose of 0.3 μM in *S. aureus* Smith, the biosynthesis of RNA, proteins, the cell wall, and fatty acids were not inhibited. These results strongly indicated that AMM is a DNA-synthesis inhibitor.

Amycolamicin selectively inhibits bacterial type II topoisomerases: In an in vivo plasmid DNA topology assay, the treatment of NOV led to an unusual mobility shift of the plasmid DNA in *E. coli* (Figure 6 and also Figure S36 in the Supporting Information). NOV is known to be a bacterial topoisomerase inhibitor, which can disturb certain topoisomerase reactions, leading to an unusual topology of the plasmid DNA detected as an unusual mobility shift. AMM also led to an unusual mobility shift of intracellular plasmid DNA, indicating that AMM also inhibited bacterial topoisomerases. On the other hand, rifamycin SV, an RNA-synthesis inhibitor, did not show any effects on the topology of plasmid

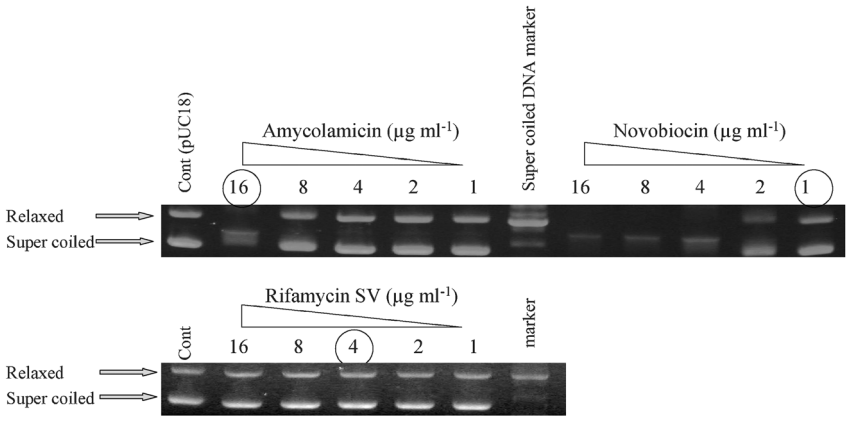

Figure 6. Effect of AMM, novobiocin, and rifamycin SV on the topology of plasmid DNA in *E. coli*. The MIC of each compound is circled. See also Figure S36 in the Supporting Information.

DNA even at doses over its MIC. When AMM was evaluated for its inhibitory activities against bacterial topoisomerases, as expected, AMM inhibited DNA gyrase and topoisomerase IV (TopoIV) with IC_{50}s of 24.4 and 6250 ng mL^{-1}, respectively (Table 3). Other inhibitors of bacterial topoisomerases, such as NOV and levofloxacin (LVFX), also inhibited the above-mentioned enzymes, but the IC_{50}s of NOV were at least two-fold higher than that of AMM, whereas LVFX inhibited TopoIV four-fold more potently than AMM and DNA gyrase four-fold weaker than AMM (Figure S37 in the Supporting Information). With respect to adverse effects of AMM on humans, the possibility of inhibiting mammalian type II topoisomerase should be evaluated, because DNA gyrase and TopoIV also belong to the type II topoisomerase family. Fortunately, AMM did not inhibit human topoisomerase II alpha even at a dose of 25000 ng mL^{-1} (Figure S38 in the Supporting Information), indicating that AMM is a specific bacterial topoisomerase inhibitor. The lethal dose of AMM in mice was higher than 250 mg kg^{-1} when administered subcutaneously. This favorable toxicological profile might be reflected by its selective inhibition toward bacterial type II topoisomerases.

Table 3. Inhibitory activities of AMM and related compounds against topoisomerases.

Test compound	IC_{50} [ng mL^{-1}]		
	E. coli		human
	DNA gyrase	DNA TopoIV	TopoIIα
amycolamicin	24.4	6250	>25000
levofloxacin	97.6	1562	>25000
novobiocin	97.6	>12500	not tested
etoposide	>8000	not tested	3125

Evaluation of possible mechanisms of resistance to amycolamicin: Aminocoumarin antibiotics, such as NOV and coumermycin A1 (COM), and quinolone antibiotics, such as levofloxacin, are known to inhibit bacterial topoisomerases. To evaluate if AMM acts at the same enzymatic site as the above-mentioned antibiotics, we constructed AMM-, NOV-, LVFX-, and COM-resistant *S. aureus* Smith strains by genetic modification of the genome and compared their susceptibilities to the above-mentioned drugs. An AMM-resistant strain of *S. aureus* Smith was selected by using continuous subculture and both the DNA gyrase (GyrA and B subunit) and TopoIV (ParC and E subunit) genes were sequenced to obtain the mutations governing the AMM resistance. The obtained strain, which is resistant to AMM, had the mutations Thr-173-Ile and Glu-201-Ala in GyrB. NOV-, LVFX-, and COM-resistant strains of *S. aureus* Smith were constructed by introducing mutations known to be involved in the resistance to the corresponding antibiotics. QRDR (quinolone-resistance determinant region) mutations such as Ser-80-Tyr and Glu-84-Lys in ParC, and Ser-84-Leu in GyrA conferred the resistance to LVFX but did not affect the MICs of AMM, NOV, and COM (Table 4). Mutation of Thr-173-Ile of GyrB caused 2-, 4-, and 512-fold resistance to AMM, NOV, and COM, respectively, and mutation of Glu-201-Ala alone did not cause AMM resistance, whereas the double mutation Thr-173-Ile and Glu-201-Ala caused a 4-fold resistance to AMM and also a 16- and a >512-fold resistance to NOV and COM, respectively. Mutations of Gln-136-Glu and Ile-175-Thr, both related to COM-resistance,[13] also impacted AMM resistance (Table 4). Although these results indicated that the target site of AMM, NOV, and COM could be similar, mutations of Asp-89-Gly and Arg-144-Ile of GyrB, known to give resistance to aminocoumarin antibiotics,[24] did not affect the AMM sensitivity, suggesting that AMM has a mode of binding to GyrB, which is distinct from coumarin and quinolone antibiotics.

Table 4. Resistance of genetically modified bacterial strains toward AMM versus common topoisomerase inhibitors.

S. aureus strains	Description	MIC [μg mL^{-1}]			
		AMM	NOV	COM	LVFX
Smith	parental	0.25	0.5	0.008	0.125
S-TI	GyrB^{Thr173Ile}	0.5	2	4	0.125
S-EA	GyrB^{Glu201Ala}	0.25	0.25	0.008	0.125
S-TIEA	GyrB^{Thr173Ile,Glu201Ala}	1	4	>4	0.125
S-RI	GyrB^{Arg144Ile}	0.25	16	2	0.125
S-DG	GyrB^{Asp89Gly}, KBD^{S}[a]	0.25	8	0.008	0.125
S-GSDG	GyrB^{Gly85Ser,Asp89Gly}	0.5	64	2	0.125
S-QEIT	GyrB^{Gln136Glu,Ile175Thr}	2	0.5	2	0.125
S-QEITLI	GyrB^{Gln136Glu,Ile175Thr,Leu455Ile}, KBD^{R}[b]	2	0.5	2	0.125
S-SY	ParC^{Ser80Tyr}	0.5	0.5	0.008	0.5
S-EK	ParC^{Glu84Lys}	0.25	0.25	0.016	0.5
S-SYSL	ParC^{Ser80Tyr}, GyrA^{Ser84Leu}	0.25	0.5	0.016	4

[a] KBD^{S} = kibdelomycin sensitive. [b] KBD^{R} = kibdelomycin resistant.

Discussion

AMM has a unique structure consisting of a *trans*-decalin skeleton with two novel sugars, that is, amycolose coupled with 3,4-dichloro-1*H*-pyrrole-2-carboxylic acid by an amide linkage and amykitanose attached to the tetramic acid by an *N*-glycosidic linkage.

Keto–enol tautomerization of the tetramic acid moiety and anomerization of the amykitanose at C-1″ would result in the equilibrium of the α and β forms of AMM in methanol. Of these isomers, the β form could not be isolated due to rapid conversion to the α form. We speculated that the anomerization was caused by the acidic conditions through an iminium intermediate of the *N*-glycoside linkage, which was associated with the tautomerization of the tetramic acid moiety and the steric effect of bulky substituents at C-2″, C-3″, and C-4″.[25]

In order to clarify the absolute chemical structure of AMM, NMR spectra, chemical degradation, and modification of its functional groups were performed. The chemical degradation of AMM gave the fragments **2**, **3α**, and **3β**. The fragment **3β** consisting of amycolose and 3,4-dichloro-1*H*-

pyrrole-2-carboxylic acid was successfully crystallized. The structural complexity of fragment **2** due to the keto–enol tautomerization of the tetramic acid and anomerization of the amykitanose in AMM could be successfully avoided by replacement of the 3″,4″-di-*O*-acyl groups with an *O*-isopropylidene group to give the separable intermediates **5α** and **5β**, which have the simplified NMR spectra of a single species in [D_5]pyridine. This process enabled successful structural analysis of compounds **6a** and **6b** by a modified Mosher's method. The stereochemistry at C-13 of the five-membered ring of the tetramic acid moiety was determined to be (*S*) configuration by degradation of AMM with periodate oxidation following acid hydrolysis according to the literature.[21] The absolute structure of the sugar **7α** obtained from AMM was clarified by comparison with the α-L-sugar **13** synthesized from α-L-(−)-fucose in six steps (Scheme S1 in the Supporting Information).

Successful determination of the entire absolute structure of AMM was achieved by a comprehensive approach, which combined degradation with synthesis. The absolute structure of AMM should provide novel insight into the analysis of the inhibitory mechanism of GyrB.

Recently, the relative structure of kibdelomycin, which is structurally closely related to AMM, has been elucidated by NMR analyses in [D_4]MeOH.[13] Though the specific rotation $[\alpha]_D^{23}$ of AMM in methanol is similar to that of kibdelomycin, the ^{1}H and ^{13}C NMR spectra of kibdelomycin in [D_4]MeOH are not identical with that of AMM as shown in Figures S11 and S12 and Table S1 in the Supporting Information (also see the Supporting Information of Ref. [13]). The ^{1}H chemical shift ($\delta = 4.14$ ppm, dd) of H-8 for the decalin moiety in AMM is clearly different from that ($\delta =$ 4.33 ppm, m) of the corresponding proton in kibdelomycin. Furthermore, all the ^{13}C signals of kibdelomycin appear in the spectrum, whereas the ^{13}C NMR signals from C-9 to C-14 of the tetramic acid moiety of AMM are not observed. All these results suggest that kibdelomycin may be a diastereomer of AMM.

We also described the antibacterial activity of AMM against various kinds of bacteria including clinically important pathogens such as *Staphylococcus aureus*, *Enterococcus faecalis*/*faecium*, *Streptococcus pneumoniae*, *Haemophilus influenzae,* and *Pseudomonas aeruginosa* as well as the analysis of the mode of action, and cross-resistance evaluations between other bacterial topoisomerase inhibitors. Despite vigorous efforts into the discovery and development of new classes of antibiotics, only three new classes of drugs (fidaxomicin, daptomycin, and linezolid) have been launched for clinical use in the past two decades. Fidaxomicin is a narrow-spectrum antibiotic developed for the treatment of *Clostridium difficile* infection.[26] Daptomycin and linezolid were approved as options for the treatment of Gram-positive pathogens such as *S. aureus* and *E. faecalis*/*faecium* and their drug-resistant strains, that is, MRSA, VRSA, and VRE.[27] Daptomycin and linezolid are not as active against Gram-negative pathogens but as they are active against Gram-positive pathogens. Therefore, ideally, a new drug should have potent antibacterial activity against not only Gram-positive pathogens but also Gram-negatives ones. AMM has potent antibacterial activity against various kinds of Gram-positive drug-resistant strains, such as MRSA, VRE, and PRSP, and some Gram-negative pathogens including BLNAR and BLPACR strains of *H. influenzae*. Our studies revealed that AMM inhibited bacterial topoisomerase, DNA gyrase, and topoisomerase IV. Distinct resistant patterns against AMM, NOV, and COM of genetically modified strains strongly suggest that these drugs have different modes of binding to GyrB. This may be derived from their structural uniqueness. Additionally, in spite of its strong inhibition of bacterial topoisomerases, AMM did not inhibit human topoisomerase II (even at a dose of 25000 ng mL^{-1}), which should limit its adverse effects in humans. These observations indicate that AMM is a very promising candidate for future drug development.

Conclusion

Screening for new antibiotics from microbial metabolites has become more difficult for several decades due to the existence of known compounds. Under these circumstances, we have used many types of drug-resistant bacteria from clinical isolates, passaged resistant strains, and genetically modified strains as test organisms for the screening. This screening system should help to eliminate known compounds and also new compounds with known modes of action, thus selecting only new compounds with novel mode of actions. During the course of our screening by using this system, we have succeeded in discovering a new compound named amycolamicin (AMM), which selectively inhibits bacterial topoisomerases. AMM has unique structural features consisting of *trans*-decalin, tetramic acid, two unusual sugars, that is, amykitanose and amycolose, and 3,4-dichloro-1*H*-pyrrole-2-carboxylic acid. Its absolute structure will offer numerous opportunities for modifications for the purpose of novel drug design.

Depending on the mutations in GyrB, the strain was slightly cross-resistant to AMM, novobiocin, and coumermycin, but not to levofloxacin, which strongly suggests that the target of AMM is the DNA gyrase B subunit, and also that the binding modes of AMM, novobiocin, and coumermycin to the target are different from each other. AMM exhibits potent antibacterial activity against current problematic drug-resistant pathogens such as MRSA, VRE, PRSP, BLNAR, and BLPACR strains of *H. influenzae*, indicating that AMM is a highly promising new drug candidate for the treatment of bacterial infections.

Experimental Section

General: Optical rotations were recorded on a P-1030 polarimeter (JASCO Inc., Tokyo, Japan). UV spectra were obtained on a U2800 spectrophotometer (Hitachi High-Technologies Corporation, Tokyo, Japan).

NMR spectra were measured with a JNM-ECA600 spectrometer (JEOL Resonance Inc., Tokyo, Japan) by using TMS as internal reference. HRESI-MS spectra were obtained on a LTQ Orbitrap XL mass spectrometer (Thermo Fisher Scientific, San Jose, CA, USA). IR spectra were recorded on a FT-210 Fourier transform infrared spectrometer (Horiba Ltd., Kyoto, Japan).

Isolation of the producing organism and taxonomy of the strains: The amycolamicin-producing organism, strain MK575-fF5, was isolated from a soil sample collected at Sendai, Miyagi prefecture, Japan. The strain MK575-fF5 formed staggered and fragmented substrate mycelia and straight to flexuous aerial mycelia. The aerial mycelia and substrate mycelia were white to light yellow orange and colorless to pale orange, respectively. Whole-cell hydrolysates of the strain contained *meso*-diaminopimelic acid, galactose, and arabinose. The strain had type PII phospholipid and MK-9(H_4) as the major components of menaquinone. The *N*-acyl-type of muramic acid in the cell wall was the acetyl type. Mycolic acid was absent. The partial 16S ribosomal RNA gene sequence (1455 bp) of the strain showed high identity with those of genus *Amycolatopsis* such as *A. balhimycina* DSM44591^T (98.8%), *A. mediterranei* JCM4789^T (98.6%) and *A. kentuckyensis* JCM12670^T (99.1%). The morphological characteristics and genetic analysis of the strain MK575-fF5 suggested that it belongs to the genus *Amycolatopsis*.[28] Therefore, the strain was designated as *Amycolatopsis* sp. MK575-fF5 (FERMP-21465).

Fermentation and purification of AMM: A slant culture of the AMM-producing organism was inoculated into a 500 mL baffled Erlenmeyer flask containing 110 mL of a seed medium consisting of 2.0% galactose, 2.0% dextrin, 1.0% Bacto soytone (Becton, Dickinson and Company, Franklin Lakes, NJ, USA), 0.5% corn steep liquor, 0.2% $(NH_4)_2SO_4$, and 0.2% $CaCO_3$ in deionized water (pH7.4 before sterilization). The culture was incubated on a rotary shaker (200 rpm) at 30°C for three days. The seed culture (2 L) was transferred into a 200 L jar fermenter, containing 100 L of a producing medium consisting of the half strength of the seed medium. The fermentation was carried out at 27°C for four days with agitation at 200 rpm and aeration of 100 NL min^{-1}.The fermentation broth (80 L) was separated into the mycelial cake and the supernatant by centrifugation. The 2.5 kg of the mycelia were extracted with 12 L of MeOH. The MeOH solutions were concentrated in vacuum to 2 L. The solution containing active compound was extracted with 6 L of EtOAc and concentrated in vacuum to yield brown oil (18 g). The brown oil was washed with 200 mL of *n*-hexane to yield a brown cake (3.3 g). The brown cake containing the active substance was purified on a SephadexLH-20 (GE Healthcare Bio-Science, Fairfield, CT, USA, column: 28 mm × 450 mm) eluted with MeOH. The active fractions were collected and concentrated in vacuo to give an orange solid (1584 mg), which was further purified by using a silica gel column with stepwise development of $CHCl_3$/MeOH/water = 100:0:0 (200 mL), 95:5:0 (450 mL), 95:5:0.25 (450 mL), and 90:10:0.5 (450 mL). The active components were eluted with $CHCl_3$/MeOH/water = 95:5:0.25 and 90:10:0.5, collected, and concentrated in vacuo to give a pale orange solid (827 mg). A small amount of the solid (54 mg) was further purified on a reversed-phase HPLC by elution with a MeOH/water = 1:1 to 1:0 linear gradient for 75 min (CAPCELL PAK C18 UG-120 5 μm, 30 mm × 250 mm, Shiseido Co., Ltd., Tokyo, Japan, flow rate = 15 mL min^{-1}). Active fractions were eluted at 55 to 60 min and collected to give a white solid (35 mg), which was suspended in EtOAc, washed with phosphate buffer (0.5 M, pH7.0), and 0.001 M aqueous HCl solution. The EtOAc extract was dried over $MgSO_4$ and filtered. The filtrate was concentrated to give 34 mg of AMM. The physical data of AMM were given in the following order: pale yellow amorphous solid; $[\alpha]_D^{23} = -36.5°$ ($c = 1$ in MeOH); ^{1}H and ^{13}C NMR data see Table 1; IR (KBr): $\tilde{\nu} = 3460$, 2930, 1730, 1610, 1540, 1460, 1380, 1310, 1240, 1080 cm^{-1}; UV/Vis (0.01 M HCl in MeOH): λ_{max} ($\log\varepsilon$) = 280 nm (4.45 mol^{-1} dm^3 cm^{-1}); (0.01 M NaOH in MeOH): λ_{max} ($\log\varepsilon$) = 248 (4.30), 277 nm (4.45 mol^{-1} dm^3 cm^{-1}); HRESI-MS (positive): *m/z* calcd for $[C_{44}H_{60}Cl_2N_4O_{14}+H]^+$: 939.3556 $[M+H]^+$; found: 939.3571.

Antibacterial activity: The minimum inhibitory concentrations (MICs) of AMM were examined by a serial agar dilution method by using Mueller–Hinton agar (Becton, Dickinson and Company) for *Enterococci*, *Streptococci*, *Staphylococcus aureus*, *Mycobacterium smegmatis*, *Escherichia coli*, *Shigella sp.*, *Salmonella enteritidis*, *Proteus sp.*, *Serratia marcescens*, *Pseudomonas aeruginosa*, *Klebsiella pneumoniae* and *Candida albicans*, and by using Mueller–Hinton agar supplemented with 5% defibrinated sheep blood (Nippon Biotest Laboratories Inc., Tokyo, Japan) under 5% CO_2 for *Streptococcus pneumoniae* and Mueller–Hinton agar enrichment supplemented with 5% Fildes enrichment peptic digest of sheep blood (Becton, Dickinson and Company) under 5% CO_2 for *Haemophilus influenzae*. The MIC was observed against acid-fasted bacteria after incubation for 42 h at 37°C, against *Candida albicans* 3147 after incubation for 18 h at 27°C, and against other bacteria after incubation for 18 h at 37°C.

Inhibition of macromolecular synthesis: Inhibition of macromolecular synthesis were assayed by measurement of the incorporation of radioactive precursors of peptidoglycan, fatty acid, DNA, RNA, and protein synthesis into the precipitate of the cell extract with 10% trichloroacetic acid (TCA) as reported previously.[29] Briefly, samples taken from the early-exponential phase (optical density at 600 nm [OD_{600}] = 0.3) of *S. aureus* Smith grown in nutrient broth were plated into 96-well plates at 90 μL per well, and then preincubated at 37°C for 5 min with antibiotics. Nutrient broth consisted of 1% polypeptone (Wako, Osaka, Japan), 1% nutrient (Kyokuto, Tokyo, Japan), and 0.2% NaCl (Wako, Osaka, Japan) in deionized water (pH7.0 before sterilization). The following radiolabeled compounds were added to the cells for the indicative assays: peptidoglycan assay: 1 μCi of *N*-acetyl-D-[1-^{3}H] glucosamine; fatty acid assay: 1 μCi of [1-^{14}C] acetate; DNA assay: 1 μCi of [methyl-^{3}H] thymidine; RNA assay: 1 μCi of [5,6-^{3}H] uridine; protein assay: 5 μCi of L-[4,5-^{3}H] leucine. All radioactive chemicals were purchased from GE Healthcare Bioscience. Mixtures were incubated for 10 min at 37°C, and then the reactions were stopped by adding an equal volume of 10% TCA. After 10 min incubation at room temperature, the solutions were transferred into 96-well filter plates (Millipore, MultiScreen$_{HTS}$, Billerica, MA, USA) and filter-washed five times with 5% TCA. After drying, the radioactivity remaining on the filter plate was counted by using a liquid-scintillation counter (Tri-Carb 2800TR, PerkinElmer, Waltham, MA, USA).

In vivo plasmid DNA topology assay: The topology of the plasmid DNA in *E. coli* was evaluated as reported previously[30] with modifications. *E. coli tolC* (efflux-deficient) strain CAG12184[31] harboring pUC18 was cultivated in Mueller–Hinton broth containing 100 μg mL^{-1} ampicillin at 37°C until mid-log phase (OD_{600} = 0.5). The cell culture was divided into 2 mL aliquots, and compound or inhibitor was added to create two-fold dilutions that spanned the MICs of each compound. The tubes were further incubated at 37°C with shaking for one hour. Plasmids were purified from the above-described cells by using a QuickLyse Miniprep Kit (QIAGEN, Valencia, CA, USA), according to the instructions of the manufacturer. The 100 ng of purified DNA was analyzed by electrophoresis along with supercoiled DNA size markers (Promega, Madison, WI, USA) in a 0.8% agarose gel. After electrophoresis, the gel was stained with ethidium bromide and photographed. Unusual DNA topology caused by inappropriate topoisomerase reactions was detected as an unusual mobility shift.

Enzyme inhibitory assay of DNA gyrase, topoisomerase IV, and human topoisomerase II: DNA gyrase and topoisomerase IV assays were performed by using the Gyrase Supercoiling assay kit (Wako, John Innes Enterprise LTD., Osaka, Japan) and the topoisomerase IV Relaxing kit (Wako, John Innes Enterprise LTD.), respectively. The 50% inhibitory concentrations (IC_{50}s) of each compound for topoisomerases were determined by measuring the densities of the bands of the digitalized data by using ImageJ free software (http://rsbweb.nih.gov/ij/). A total of 30 mL of the gyrase supercoiling reaction mixture, which contained gyrase (*E. coli,* $GyrA_2B_2$) (1 unit), 7 μM Tris-HCl (pH 7.5), 4.8 mM KCl, 0.4 mM $MgCl_2$, 0.4 mM dithiothreitol (DTT), 0.36 mM spermidine, 0.2 mM ATP, 20 μg mL^{-1} albumin, 1.3% (v/v) glycerol, and 400 ng relaxed pBR322 DNA was incubated at 37°C for 30 min and then terminated by addition of 5 μL of stop buffer (5% sarkosyl, 0.0025% bromophenol blue, 25% glycerol), followed by electrophoretic analysis in 0.8% agarose gels. Topoisomerase IV relaxing assays were performed as follows. A total of 30 μL of the reaction mixture, consisting of topoisomerase IV (*E. coli,* $ParC_2E_2$) (1 unit), 40 mM HEPES/KOH (pH 7.6), 100 mM potassium glu-

tamate, 10 mM magnesium acetate, 10 mM DTT, 4 $\mu g\,mL^{-1}$ tRNA, 2 mM ATP, 50 $\mu g\,mL^{-1}$albumin, and 400 ng supercoiled pBR322 DNA was incubated at 37 °C for 30 min and then terminated by addition of 5 μL of stop buffer (5% sarkosyl, 0.0025% bromophenol blue, 25% glycerol), followed by electrophoretic analysis in 0.8% agarose gels. The human topoisomerase II decatenation assay was performed by using the topoisomerase II assay kit (TopoGEN, Inc. Port Orange, FL, USA) using human DNA topoisomerase II alpha of the p170 form (TopoGEN, Inc.). An aliquot of 30 μL of the decatenation assay mixture, which contained 50 mM Tris-HCl (pH 8.0), 150 mM NaCl, 10 mM $MgCl_2$, 5 mM ATP, 0.5 mM DTT, 30 $\mu g\,mL^{-1}$ bovine serum albumin, and 0.2 μg kinetoplast DNA (kDNA) was incubated at 37 °C for 30 min and then terminated by addition of 5 μL of stop buffer (5% sarkosyl, 0.0025% bromophenol blue, 25% glycerol), followed by electrophoretic analysis in 0.8% agarose gels with linear kDNA markers.

Construction of *S. aureus* Smith mutants resistant to DNA gyrase inhibitors: An AMM-resistant strain of *S. aureus* Smith was selected by using continuous subculture and both the DNA gyrase (GyrA and B subunit) and topoisomerase IV (ParC and E subunit) genes were sequenced to obtain the mutations responsible for the resistance. The *gyrA, gyrB*, or *parC* structural gene of *S. aureus* Smith was amplified by PCR and cloned into the *E. coli–S. aureus* shuttle vector pHY300PKL (TaKaRa Bio Inc., Shiga, Japan) containing the tetracycline-resistant gene. Subsequently, the obtained or known missense mutations were induced in the corresponding gene of this plasmid by using a recombination PCR method[32] with PrimeSTAR GXL DNA polymerase (TaKaRa Bio Inc.). The resulting plasmids were introduced into *S. aureus* Smith by electroporation as previously reported,[33] with slight modifications and selected by tetracycline. The obtained transformants were challenged with the corresponding antibiotic and resistant mutants were selected. These mutants were then confirmed by their drug resistance, and the sequences of the *gyrB* gene on their genome. Because the mutated *gyrB* gene on the plasmid did not have a promoter, the transformants could survive under the presence of the drug only when the *gyrB* gene on the genome was replaced with the mutated gene on the plasmid. The MICs of AMM, NOV, COM, and LVFX against the above-constructed strains were determined by a standard microbroth dilution method by using nutrient broth.

Acknowledgements

The authors are grateful to the National bioresource project: *E. coli*, the National institute of genetics, Japan for providing the *E. coli tolC* (efflux-deficient) strain CAG12184. We are indebted to Dr. Hiroyasu Sato at Rigaku Corporation for the X-ray crystallographic analysis of **3β**. We express thanks to Dr. Tomoyuki Kimura for assistance with the X-ray analysis. We thank Yumiko Kubota and Yoshiko Koyama for valuable discussion about the structure determination. We also thank Yuichi Kasahara for technical assistance with the fermentation of AMM.

[1] L. D. Saravolatz, J. Pawlak, L. B. Johnson, *Int. J. Antimicrob. Agents* **2010**, *36*, 69–72.
[2] R. Leclercq, E. Derlot, M. Weber, J. Duval, P. Courvalin, *Antimicrob. Agents Chemother.* **1989**, *33*, 10–15.
[3] S. Chang, D. M. Sievert, J. C. Hageman, M. L. Boulton, F. C. Tenover, F. P. Downes, S. Shah, J. T. Rudrik, G. R. Pupp, W. J. Brown, D. Cardo, S. K. Fridkin, *N. Engl. J. Med.* **2003**, *348*, 1342–1347.
[4] S. C. A. Meijvis, J. C. Grutters, S. F. Thijsen, G. T. Rijkers, D. H. Biesma, H. Endeman, *Neth. J. Med.* **2011**, *69*, 21–26.
[5] N. Chiba, R. Kobayashi, K. Hasegawa, M. Morozumi, E. Nakayama, T. Tajima, S. Iwata, K. Ubukata, *J. Antimicrob. Chemother.* **2005**, *56*, 756–760.
[6] N. Bruinsma, K. G. Kristinsson, S. Brozwaer, P. Schrijnemakers, J. Degener, E. Tiemersma, W. Hryniewics, J. Monen, H. Grundmann, *J. Antimicrob. Chemother.* **2004**, *54*, 1045–1050.
[7] P. Littauer, M. Sangvik, D. A. Caugant, E. A. Høiby, G. S. Simonsen, A. Sundsfjord, *J. Clin. Microb.* **2005**, *43*, 2125–2132.
[8] S. Bae, J. Lee, E. Kim, S. Lee, J. Yu, Y. Kang, *Antimicrob. Agents Chemother.* **2010**, *54*, 65–71.
[9] R. J. Fass, *Antimicrob. Agents Chemother.* **1983**, *24*, 568–574.
[10] I. Hayakawa, S. Atarashi, S. Yokohama, M. Imamura, K. Sakano, M. Furukawa, *Antimicrob. Agents Chemother.* **1986**, *29*, 163–164.
[11] I. Momose, S. Hirosawa, H. Nakamura, H. Naganawa, H. Iinuma, D. Ikeda, T. Takeuchi, *J. Antibiot.* **1999**, *52*, 787–796.
[12] D. R. Schroeder, K. L. Colson, S. E. Klohr, M. S. Lee, J. A. Matson, *J. Antibiot.* **1996**, *49*, 865–872.
[13] J. W. Phillips, M. A. Goetz, S. K. Smith, D. L. Zink, J. Polishook, R. Onishi, S. Salowe, J. Wiltsie, J. Allocco, J. Sigmund, K. Dorso, S. Lee, S. Skwish, M. de la Cruz, J. Martin, F. Vicente, O. Genilloud, J. Lu, R. E. Painter, K. Young, K. Overbye, R. G. Donald, S. B. Singh, *Chem. Biol.* **2011**, *18*, 955–965.
[14] B. A. Sherer, K. Hull, O. Green, G. Basarab, S. Hauck, P. Hill, J. T. Loch III, G. Mullen, S. Bist, J. Bryant, A. Boriack-Sjodin, J. Read, N. DeGrace, M. Uria-Nickelsen, R. N. Illingworth, A. E. Eakin, *Bioorg. Med. Chem. Lett.* **2011**, *21*, 7416–7420.
[15] S. Tohyama, Y. Takahashi, Y. Akamatsu, *J. Antibiot.* **2010**, *63*, 147–149.
[16] P. S. Steyn, P. L. Wessels, *Tetrahedron Lett.* **1978**, *19*, 4707–4710.
[17] B. J. L. Royles, *Chem. Rev.* **1995**, *95*, 1981–2001.
[18] I. Ohtani, T. Kusumi, Y. Kashman, H. Kakisawa, *J. Am. Chem. Soc.* **1991**, *113*, 4092–4096.
[19] Ok. Kwang-dae, Y. Takagi, T. Tsuchiya, S. Umezawa, H. Umezawa, *Carbohydr. Res.* **1987**, *169*, 69–81.
[20] Y. Takagi, N. Kobayashi, T. Tsuchiya, S. Umezawa, T. Takeuchi, K. Komuro, C. Nosaka, *J. Antibiot.* **1989**, *42*, 1318–1320.
[21] H. Ikeda, N. Matsumori, M. Ono, A. Suzuki, A. Isogai, H. Nagasawa, S. Sakuda, *J. Org. Chem.* **2000**, *65*, 438–444.
[22] K. Fujii, Y. Ikai, H. Oka, M. Suzuki, K. Harada, *Anal. Chem.* **1997**, *69*, 5146–5151.
[23] H. Hashizume, H. Adachi, M. Igarashi, Y. Nishimura, Y. Akamatsu, *J. Antibiot.* **2010**, *63*, 279–283.
[24] M. Fujimoto-Nakamura, H. Ito, Y. Oyamada, T. Nishino, J. Yamagishi, *Antimicrob. Agents Chemother.* **2005**, *49*, 3810–3815.
[25] H. S. Isbell, H. L. Frush, *J. Org. Chem.* **1958**, *23*, 1309–1319.
[26] C.-H. Liao, W.-C. Ko, J.-J. Lu, P.-R. Hsueh, *Antimicrob. Agents Chemother.* **2012**, *56*, 3943–3949.
[27] L. A. Jevitt, A. J. Smith, P. P. Williams, P. M. Raney, J. E. McGowan, Jr., F. C. Tenover, *Microb. Drug Resist.* **2003**, *9*, 389–393.
[28] M. P. Lechevalier, H. Prauser, D. P. Labeda, J. S. Ruan, *Int. J. Syst. Bacteriol.* **1986**, *36*, 29–37.
[29] H. Hashizume, R. Sawa, S. Harada, M. Igarashi, H. Adachi, Y. Nishimura, A. Nomoto, *Antimicrob. Agents Chemother.* **2011**, *55*, 3821–3828.
[30] T. H. Grossman, D. J. Bartels, S. Mullin, C. H. Gross, J. D. Parsons, Y. Liao, A. L. Grillot, D. Stamos, E. R. Olson, P. S. Charifson, N. Mani, *Antimicrob. Agents Chemother.* **2007**, *51*, 657–666.
[31] M. Singer, T. A. Baker, G. Schnitzler, S. M. Deischel, M. Goel, W. Dove, K. J. Jaacks, A. D. Grossman, J. W. Erickson, C. A. Gross, *Microbiol. Rev.* **1989**, *53*, 1–24.
[32] D. H. Jones, *Genome Res.* **1994**, *3*, S141–S148.
[33] S. Schenk, R. A. Laddaga, *FEMS Microbiol. Lett.* **1992**, *94*, 133–138.

Received: July 25, 2012
Published online: November 5, 2012

